

Demography of high redshift AGN

Fabrizio Fiore¹, Simonetta Puccetti², Smita Mathur³

¹*INAF - Osservatorio Astronomico di Roma*

²*ASI SDC and*

³*Ohio State University, USA*

(Dated: June 14, 2018)

High redshift AGN holds the key to understand the early structure formation and to probe the Universe during its infancy. We review the latest searches for high- z AGN in the deepest X-ray field so far, the Chandra Deep Field South (CDFs) 4 Msecond exposure. We do not confirm the positive detection of a signal in the stacked Chandra images at the position of $z \sim 6$ galaxies recently reported by Treister and collaborators [29]. We present $z > 3$ X-ray sources number counts in the 0.5-2 keV band obtained joining CDFS faint detections [13] with Chandra-COSMOS and XMM-COSMOS detections. We use these number counts to make predictions for surveys with three mission concepts: Athena, WFXT and a Super-Chandra.

I. INTRODUCTION

The study of high redshift AGN holds the key to understand the early structure formation and probe the Universe during its infancy. High- z AGN can be used to investigate important issues such as: 1) the evolution of the correlations between the black hole mass and the galaxy properties (see e.g. [17] and references therein); 2) the AGN contribution to the re-ionization, heating of the Inter-Galactic Medium and its effect on structure formation (e.g. [2, 23] and references therein); 3) scenarios for the formation of the black hole (BH) seeds, which will eventually grow up to form the super-massive black holes (SMBHs) seen in most galaxy bulges (e.g. [30]); 4) investigate the physics of accretion at high- z : is BH growth mainly due to relatively few accretion episodes, as predicted in hierarchical scenarios (see e.g. [6] and references therein), or by the so called chaotic accretion (hundreds to thousands of small accretion episodes, [16])? 5) BHs, being the structures with the fastest (exponential) growth rate, can be used to constrain both the expansion rate of the Universe and the growth rate of the primordial perturbations at high- z , of competing cosmological scenarios [12, 18]. 6) The slope of the high- z AGN luminosity function and of the SMBH mass function strongly depend on the AGN duty cycle, and therefore their measure can constrain this critical parameter. In turn, the AGN duty cycle holds information on the AGN triggering mechanisms. The evaluation of the evolution of the AGN duty cycle can thus help in disentangling among competing scenarios for AGN triggering and feeding [13].

Large area optical and near infrared surveys such as the SDSS, the CFHQS, the NOAO DWFS/DLS and the UKIDSS surveys have already been able to discover large samples of $z > 4.5$ QSOs (e.g. [14, 27]) and about 50 QSOs at $z > 5.8$ (e.g. [15, 24, 32]). The majority of these high- z AGN are broad line, unobscured, high luminosity AGN. They are likely the tips of the iceberg of the high- z AGN population. Lower luminosity and/or moderately obscured AGN can, in principle, be detected directly in current and future X-ray surveys. Dedicated searches for high- z AGN using both deep and wide area X-ray surveys and a multi-band selection of suitable candidates can increase the number of high- z AGN by a factor > 10 . In particular, it should be possible to find hundreds rare high- z , high luminosity QSOs, in both the all sky and deep eROSITA surveys (the 0.5-2 keV flux limit of the all sky survey being the order of 10^{-14} erg/cm²/s, while that of the deep survey, covering hundreds deg², should be 2-3 times deeper) with a selection function much less biased than optical surveys. To constrain the faint end of the high- z AGN luminosity function, and therefore the shape of the luminosity function and of the SMBH mass function, we need to best exploit current and future deep surveys. The Chandra Deep Field South is today the *premiere* field, with its 4 Msec and 3 Msec exposures obtained by Chandra and XMM respectively, since 1999. Three different approaches have been so far applied to this field: a) direct detection of sources in X-ray maps (e.g. [33]); b) search for X-ray emission at the position of candidate high- z galaxies selected in the red and near infrared bands [13]; c) stacking of X-ray counts at the position of candidate high- z galaxies [29]. Here we review all three methods and give state of the art number counts of high- z AGN at faint fluxes. We use these number counts to predict the number of high- z AGN in possible future deep X-ray surveys. A $H_0 = 70$ km s⁻¹ Mpc⁻¹, $\Omega_M = 0.3$, $\Omega_\Lambda = 0.7$ cosmology is adopted throughout.

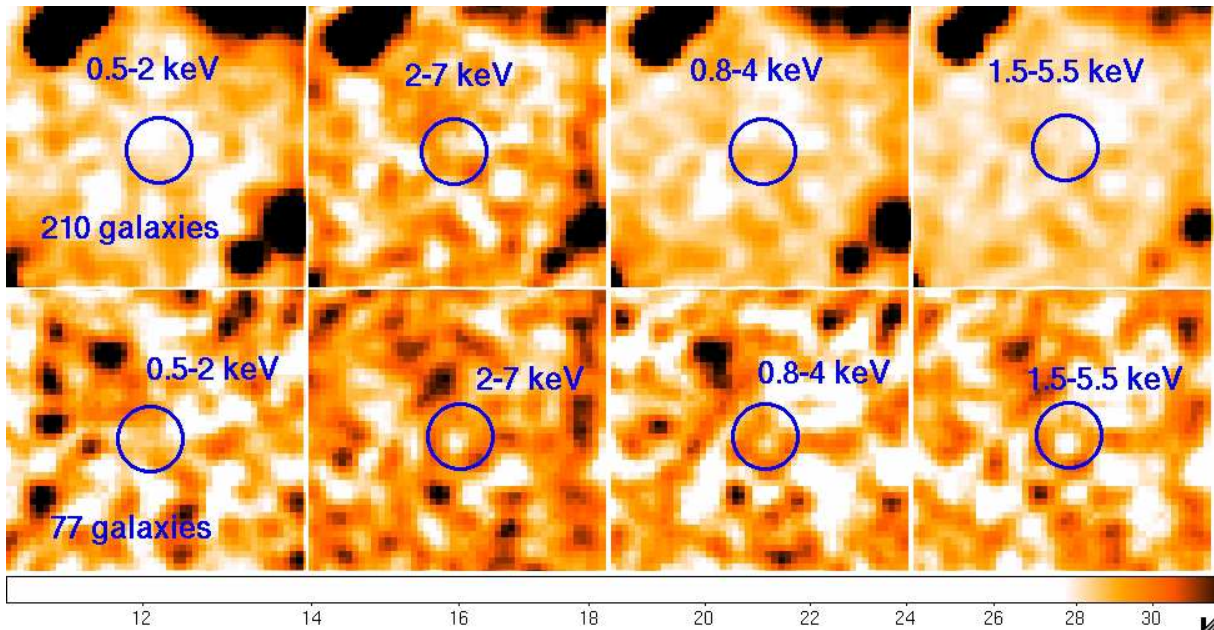


FIG. 1: Stacks of Chandra images at the position of 210 and 77 Bouwens et al. [3] candidate $z \sim 6 - 7$ galaxies in four energy bands: 0.5-2 keV, 2-7 keV, 0.8-4 keV and 1.5-5.5 keV.

II. STACKING ANALYSIS OF CANDIDATE HIGH-Z GALAXIES

Recently Treister et al. [29] published a positive detection of X-ray counts in stacked Chandra images obtained adding together the X-ray counts at the position of 197 candidate high- z galaxies at $z \sim 6$ in the CDFS and CDFN [3]. They find 5σ and 6.8σ detections in the soft 0.5-2 keV and hard 2-8 keV bands. Since the 2-8 keV flux they detect is about 9 times the 0.5-2 keV flux they infer that the majority of these faint high- z galaxies host highly obscured, Compton thick AGN. The total rest frame 2-10 keV luminosity density implied by the Treister [29] result is 1.6×10^{46} ergs/s/deg² at $z \sim 6$. In contrast, Fiore et al. [13] analyzed X-ray counts at the position of the same Bouwens et al. [3] $z \sim 6$ galaxies in the CDFS finding just one marginal detection. Fiore et al. [13] find that the $z \sim 6$ luminosity function can be modeled using the standard double power law shape:

$$\frac{d\Phi(L_X)}{d\text{Log}L_X} = A[(L_X/L_*)^{\gamma_1} + (L_X/L_*)^{\gamma_2}]^{-1}. \quad (1)$$

with $L^* = 2 \times 10^{44}$ ergs/s, $\gamma_1=0.8$ and $\gamma_2=3.4$ (the faint end slope is not truly constrained). By integrating this luminosity function above a luminosity of 10^{42} erg/s one obtains a total rest frame 2-10 keV luminosity density at $z \sim 6$ of 5.6×10^{45} ergs/s/deg², a value ~ 2.8 times smaller than that reported by Treister et al. [29]. We investigated this discrepancy between the Treister [29] and Fiore [13] results. Once again we considered the Bouwens et al. [3] sample of 371 candidate $z \sim 6$ galaxies in the CDFS. Some of these galaxies happen to lie close to bright X-ray sources identified with galaxies at a different redshift, and must therefore be excluded from the analysis. We considered two exclusion radii, one similar to that used by Treister [29], i.e. 22 arcsec, and another less conservative, 10 arcsec. In both cases we used the new Xue et al. [33] catalog of 740 directly detected X-ray sources. We considered sources at an offaxis angle < 8 arcmin, to avoid the inclusion of sources observed with a too wide PSF. We also considered only one galaxy when we find 2 or more within 2 arcsec, not to count twice the contribution from each single object. We finally excluded from the samples $z \sim 6$ galaxies closer than 2 arcsec from lower redshift galaxies brighter than $z_{\text{mag}} = 25$, which may contaminate the high redshift stacks. The final samples include 210 galaxies (10 arcsec exclusion radii) and 77 galaxies (22 arcsec exclusion radii). We performed stacks of Chandra counts at the position of these galaxies in four energy bands: 0.5-2 keV, 2-7 keV, 0.8-4 keV and 1.5-5.5 keV. The total exposure times for

TABLE I: 3σ count rates upper limits

sample	0.5-2 keV 10^{-7} cts/s	2-7 keV 10^{-7} cts/s	0.8-4 keV 10^{-7} cts/s	1.5-5.5 keV 10^{-7} cts/s
210 galaxies	3.4	5.8	6.2	6.2
77 galaxies	5.9	9.7	9.6	10.1

the two sample are $\sim 2.3 \times 10^8$ seconds (77 galaxies) and $\sim 6.3 \times 10^8$ seconds (210 galaxies). Fig. 1 shows the stacked images for the two samples in the four energy bands. We do not find a significant signal at the position of the galaxies in any of these images. Table 1 gives the PSF corrected 3σ count rate upper limits from the counts collected in boxes of 5 arcsec side (area of 100 original pixels). As a comparison, Treister et al. [29] report a count rate $3.4 \pm 0.7 \times 10^{-7}$ counts/s in the 0.5-2 keV band and $8.8 \pm 1.3 \times 10^{-7}$ counts/s in the 2-8 keV band. Our more stringent upper limits are obtained for the 210 galaxy sample in the 0.5-2 keV and 2-7 keV bands. These are respectively comparable and 1.5 times lower than the Treister [29] claimed detections.

We can convert our count rate upper limits to a limit to the rest frame 2-10 keV luminosity density following [29]. We find a 3σ limit of $\sim 10^{46}$ ergs/s/deg², lower than the [29] feature, but about twice the luminosity density estimated by Fiore et al. [13].

We recall that our analysis applies to the CDFS field alone, while the [29] result applies to the joined CDFS and CDFN area. At least part of the discrepancy between Treister et al. [29] and our analysis could therefore be due to cosmic variance. We also recall that for the sake of robustness our stacking analysis is the simplest possible: counts at the position of galaxies are added together, and aperture photometry is performed on the stacked images without any optimization for off-axis dependent PSF. Background is estimated in nearby regions, and, unlike [29], no removal of positive fluctuations is performed. While this simple technique does not probably push the detection to the limit, it nevertheless produced valuable results in the past when applied to samples of candidate, faint, Compton thick AGN [10, 11].

III. HIGH-Z AGN NUMBER COUNTS

The analyses on the CDFS, CDFN, EGS and COSMOS fields provide samples of individual sources detected, and therefore X-ray number counts of faint high-z sources can be easily computed from these samples. Fig. 2 show $z > 3$ number counts from a compilation of surveys: the Fiore et al. [13] survey of the ERS and GOODS fields, and the Brusa et al. and Civano et al [4, 5] XMM and Chandra surveys of the COSMOS field. Black solid lines are model number counts obtained by converting the [13] luminosity functions. At the flux limits reached by the deepest Chandra exposure (4 Mseconds) there are $> 1000 z > 3$ AGN/deg², several hundreds of $z > 4$ AGN/deg², $> 100 z > 5$ AGN/deg², $20-100 z > 5.8$ AGN/deg² (the uncertainty on the latter number is so large because it is based on just 2 candidate $z > 5.8$ galaxies detected by Chandra in the small ERS field). It is clear that to obtain a more robust demography of the $z > 6$ sky a search in a much wider area, such as the CANDELS area, is mandatory, and requires spectroscopic confirmation of the X-ray emitting, candidate $z > 6$ galaxies. The CANDELS deep and wide surveys cover a total of 130 arcmin² and 670 arcmin² to a depth of $H=27.8$ and $H \sim 26.5$ respectively. As a comparison, the ERS survey covers an area of 50 arcmin² to a depth of $H \sim 27$. The two candidate $z > 6$ ERS galaxies detected by Chandra in the ERS field are faint, $H=26.6$ and $H=27$ sources. The GOODS source with $z > 7$ in the Luo et al. [21] catalog has $H=27.6$. The other $z > 6$ ERS galaxy with a marginal X-ray detection is brighter, $H=23.8$. In summary, we expect 1-5 $z > 6$ AGN in CANDELS deep and 4-20 $z > 6$ AGN in CANDELS wide. However, we note that a fraction of these sources will be at the limit, or below, the H band sensitivity threshold of the wide survey. As of today Chandra has spent of the order of 8 Mseconds on the CANDELS fields, most of them on the CANDELS deep fields. To reach the sensitivity to detect the faint $z > 6$ AGN in the wide area, additional 5-6 Mseconds are needed. This is within reach of the Chandra observatory in the next few years. To make further progresses with Chandra, i.e. quantitatively probe the first generation of accreting SMBH, which would allow putting stringent constraints on SMBH formation models [1, 19, 22, 31], and accretion scenarios [6, 9, 16, 30], would require at least triple the exposure times, i.e. 30-40 Mseconds on deep surveys. While this is certainly extremely expensive, it is not technically unfeasible.

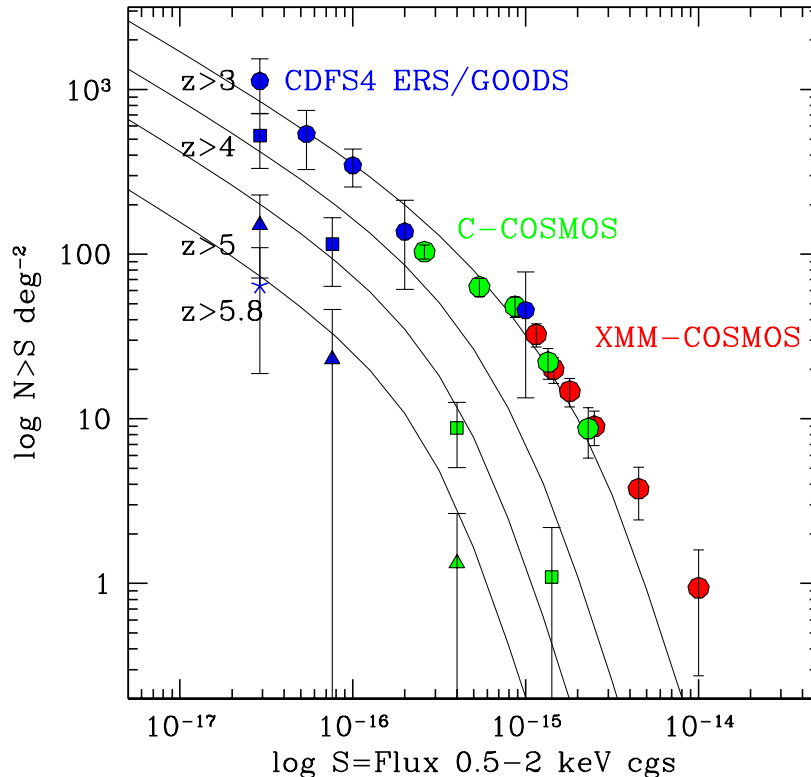


FIG. 2: Faint X-ray sources number counts in the 0.5-2 keV band. Blue points are from X-ray detections at the position of ERS and GOODS-MUSIC $z > 3$ galaxies [13]; green points are from Chandra-COSMOS [5]; red points are from XMM-COSMOS [4]. Circles = $z > 3$ sources, squares = $z > 4$ sources, triangles = $z > 5$ and star = $z > 5.8$ sources. The thin solid curves are model number counts based on the best fit high- z luminosity functions presented in [13].

IV. PREDICTION FOR FUTURE SURVEYS

The Chandra limiting problem is that its sensitivity is very good on axis, but degrades quickly at off-axis angles higher than a few arcmin, making difficult and expensive in terms of exposure time to cover with good sensitivity area larger than a few hundred arcmin². A significant leap forward in the field would then be obtained by an instrument capable of reaching the Chandra Msecond exposure, on axis sensitivity (i.e. flux limits in the range $1 - 3 \times 10^{-17}$ erg/cm²/s) but on a factor of > 10 wider field of view (FOV). We consider here three possible mission concepts, making predictions on the number of $z > 4$, $z > 5$ and $z > 6$ faint x-ray sources based on our best knowledge today, i.e. the number counts in Fig. 2 and the luminosity functions in [13].

1) Athena. This is a proposal for L class mission in the framework of the ESA Cosmic Vision program. The baseline mission concept foresees an effective area for imaging of the order of half square meter at 1-2 keV, a mirror PSF with half power diameter HPD ~ 10 arcsec (requirement, 5 arcsec goal), focal length 11m, FOV=0.17 deg² (25 \times 25 arcmin). The observatory should be launched on a high Earth orbit (HEO) or a L2 orbit, and therefore a rather high internal background is predicted (similar to the internal background measured by the instruments on board XMM and Chandra, which are flying on HEO).

2) WFXT. The concept for a wide field X-ray telescope is quite old, the first idea dating mid 90', and it evolved considerably over the years. We assumed a configuration similar to that in [25], i.e. an effective area of $>$ half square meter at 1-2 keV, split in three mirror units, with HPD=10 arcsec (requirement, goal

TABLE II: Predicted number of faint, high- z X-ray sources

Mission concept	PSF HPD	Mosaics	total FOV	$z=4-5$	$z=5-5.8$	$z > 5.8$
	arcsec		deg ²	LX($z=5$)	LX($z=6$)	LX($z=7$)
Athena*	10	60x0.2Msec	10	940 >43.3	480 >43.5	250 >43.6
Athena*	5	6x2Msec	1.0	360 >42.5	210 >42.6	125 >42.8
Athena	5	40x0.3Msec	7.0	1100 >43	650 >43.1	360 >43.2
WFXT*	10	24x0.5Msec	24	2300 >43.2	1300 >43.4	600 >43.5
WFXT*	5	4x3Msec	4	1200 >42.5	700 >42.6	400 >42.8
WFXT	5	60x0.2Msec	60	6000 >43.35	3200 >43.4	1600 >43.5
S-Chandra	2	6x2Msec	0.6	310 >42.2	185 >42.3	110 >42.5
S-Chandra	2	24x0.5Msec	2.4	390 >43	220 >43.1	125 >43.2
S-Chandra	1	2x6Msec	0.2	175 >41.8	100 >42.0	65 >42
S-Chandra	1	6x2Msec	0.6	350 >42.1	210 >42.2	120 >42.4

* close to confusion limit (40 beams per source).

5 arcsec), and 5.5m focal length. Each mirror unit is feeding a focal plane camera with FOV ~ 1 deg². We assumed that the observatory is in a low Earth orbit (LEO), ensuring a low internal background (similar to that of the instrument on board Swift and Suzaku, which are flying on a LEO).

3) Super-Chandra. This is a straw-man design for a mission with imaging capabilities comparable to Chandra (i.e. arcsec HPD), but using high throughput light weight mirrors (a concept pioneered by Martin Elvis and Pepi Fabbiano some 15 years ago [7]). Good imaging capabilities using thin glass or nickel shells may be obtained by correcting the shell shape with actuators. Studies of active X-ray mirrors have been performed in the past with good results (see www.mssl.ucl.ac.uk/sxoptics). A SPIE conference had been devoted to active X-ray mirrors in 2010 (Proceedings of SPIE 7803). Active X-ray optics have been foreseen for extremely large throughput, sub-arcsec future missions like Generation-X [8, 26] or, more recently, for a square meter, sub-arcsec mission (Vikhlinin et al. 2011, HEAD meeting). Here we assume a more modest throughput (~ 3000 cm² at 1-2 keV) and PSF (1-2 arcsec HPD). We also assumed a limited FOV (0.1 deg²) and a LEO, which ensures a low internal background.

By using the above parameters we computed on axis sensitivities as a function of the observing time (assuming a signal to noise ratio of 3 for source detection). To make realistic predictions for the number of high- z AGN expected, we assume that the effective area decreases linearly from the center to the limit of the FOV by 50%. The background includes particle induced internal background, as measured on HEO and LEO, cosmic X-ray background (CXB), and low temperature thermal X-ray background due to the local superbubble. The internal background dominates over the X-ray background (CXB and the local superbubble) above 0.5 keV in a HEO. Conversely, on LEO the local superbubble dominates below 1 keV. We finally assumed a total net observing time of 12 Mseconds devoted to surveys, split in several shorter observations, to cope with source confusion and optimize the detection of $z > 5$ sources with 2-10 keV luminosity $\gtrsim 10^{42}$ ergs/s. The standard criterion for source confusion (40 beams per source) translates in a flux limit for source confusion of $\sim 6 \times 10^{-17}$ erg/cm²/s in the 0.5-2 keV band for PSF HPD=10 arcsec and just above 10^{-17} erg/cm²/s for HPD=5 arcsec. Source confusion is not an issue for realistic exposure times for a PSF with HPD=2 arcsec or below.

To estimate the faint X-ray sources number density we used the model number counts in Fig 2, based on the luminosity functions presented in [13]. We conservatively assumed a faint-end slope of the X-ray luminosity functions $\gamma_1=0.6$. Table 2 gives the predicted number of $z=4-5$, $z=5-5.8$ and $z > 5.8$ sources, along with their minimum 2-10 keV luminosity for several indicative mosaics for the three mission concepts briefly described above.

It must be noted that the uncertainties on the number of sources in Table 2 is large. It is at least a factor of two at $z=4-6$ and even bigger at $z > 6$ (factor of 3 lower limit and a factor of 2 upper limit). The obvious message of Table 2 is that a wide field greatly helps in searching for high- z AGN. This is probably the only solution to collect samples of thousands X-ray AGN at $z > 4$. However, even a PSF as good as 5 arcsec HPD does not allow searching for sources fainter than 10^{43} ergs/s at $z > 5-7$. This means that only a mission with Chandra-like PSF but much higher throughput ($> 5 \times$ Chandra effective area at 1-2 keV) would be able to target normal starforming galaxies and mini-quasars at $z=6-7$. On one hand, a 2-10 keV luminosity of 10^{42} ergs/s at $z=7$, reachable by extradeep exposures with a 1 arcsec PSF Super-Chandra, would be produced

by a 7×10^5 SMBH emitting at its Eddington luminosity (assuming a bolometric correction of 10). Even smaller masses may be probed, if the accretion is super-Eddington. A Super-Chandra would then be able to directly search for the first generation of SMBH produced by monolithic collapse of $\gtrsim 10^5 M_{\odot}$ gas clouds to BH [1, 19, 20, 31]. On the other hand, $L(2-10)=10^{42}$ ergs/s is also produced by galaxies which form stars at a rate of $\gtrsim 200 M_{\odot}/\text{yr}$. Since at such high redshifts X-ray emission should mainly be due to high mass X-ray binaries, X-ray high- z galaxies could then be used to constrain the initial mass function at the epoch of galaxy formation. A Super-Chandra would then be able to open two brand-new fields in structure formation. Of course it is not casual that the considered configuration for a Super-Chandra is able to reach these goals. Going back from scientific requirements to mission parameters, the goal of detecting sources with a 2-10 keV luminosity of $\sim 10^{42}$ at $z \sim 7$, in feasible exposure times, requires an effective area $\sim 3000 \text{ cm}^2$, given a PSF HPD ~ 1 arcsec and assuming a LEO low internal background.

Unfortunately a Super-Chandra is beyond the horizon of the present decade, both because technological and programmatic issues. Furthermore, it is not clear whether a WFXT is truly feasible with such huge 1 deg^2 FOV and large throughput, and in any case it does not appear to be a priority in the latest US Decadal Survey (http://sites.nationalacademies.org/bpa/BPA_049810) nor in the ESA Cosmic Vision program. Conversely, Athena is a study mission for an L class mission in the framework of the ESA Cosmic Vision program. A decision for CV L class mission should be taken in February 2012. If positive, Athena could be implemented for the first years of the next decade. Although not reaching exquisite, Chandra-like image quality, nor extra-large field of view, Athena would be able to give a substantial contribution on the knowledge of the high- z Universe, with hundreds to a thousand $z > 4$ X-ray AGN (an improvement by a factor 10-100 with respect to today situation) and tens to hundreds $z > 5.8$ X-ray selected AGN (today there are only 3-4 candidate $z > 6$ X-ray selected AGN in the literature [13, 21, 28]).

Acknowledgments

This work was supported by ASI/INAF contracts I/024/05/0 and I/009/10/0. This work is based on observations made with NASA X-ray observatory Chandra. We thank the Chandra Director's office for allocating the time for these observations. X-ray data were obtained from the archive of the Chandra X-ray Observatory Center, which is operated by the Smithsonian Astrophysical Observatory.

-
- [1] Begelman M.C. 2010, MNRAS, 402, 673
 - [2] Boutsia K. et al. 2011, ApJ, in press, arXiv:1104.5237
 - [3] Bouwens R.J., Illingworth G.D., Blakeslee J.P., Franx M. 2006, ApJ, 653, 53
 - [4] Brusa M. et al. 2009, ApJ, 693, 8
 - [5] Civano F. et al. 2011, ApJ, in press, arXiv:1103.2670
 - [6] Dotti M., Volonteri M., Perego A., Colpi M., Ruzsowski M., Haardt F. 2010, MNRAS, 402, 682
 - [7] Elvis M., Fabbiano G. 1996, arXiv:9611178
 - [8] Elvis M. et al. 2006, SPIE, arXiv:0608533
 - [9] Fanidakis N., Baugh, C. M., Benson A. J., Bower R. G., Cole S., Done C., & Frenk C. S. 2011, MNRAS, 410, 53
 - [10] Fiore F. et al. 2008, ApJ, 672, 94
 - [11] Fiore F. et al. 2009 ApJ, 693, 447
 - [12] Fiore F. 2010, AIP Conference Proceedings, Volume 1248, pp. 373-380, arXiv:1002.3538
 - [13] Fiore F. et al. 2011, A&A, in press, arXiv:1109.2888
 - [14] Glikman E., Djorgovski S. G., Stern D., Dey A. Jannuzi B.T. Lee K-S 2011, ApJ, 728 L26
 - [15] Jiang L. et al., 2009, AJ, 138, 305
 - [16] King A.R., Pringle J.E., Hofmann J.A. 2008, MNRAS, 385, 1621
 - [17] Lamastra A., Menci N., Maiolino R., Fiore F., Merloni A. 2010, MNRAS, 405, 29
 - [18] Lamastra A., Menci N., Fiore F., Di Porto C. Amendola L. 2011, MNRAS, submitted
 - [19] Lodato G. & Natarajan P. 2006, MNRAS, 371, 1813
 - [20] Lodato G. & Natarajan P. 2007, MNRAS, 377, L64
 - [21] Luo B., et al. 2010, ApJS, 187, 560
 - [22] Madau P., Rees M.J. 2001, ApJ, 551, L27
 - [23] Mitra S., Choudhury T.R., Ferrara A. 2011, MNRASsubmitted, arXiv:1106.4034

- [24] Mortlock D.J et al. 2011, Nature, in press, arXiv:1106:6088
- [25] Murray S. et al. 2009, arXiv:0903:5272
- [26] O'Dell, S.L. et al. 2010, SPIE Conference 7803 "Adaptive X-ray Optics", arXiv:1010:4892
- [27] Richards G. T. et al, 2006, ApJS, 166, 470
- [28] Salvato M. et al. 2011, ApJ, in press, arXiv:1108:6061
- [29] Treister E., Schawinski K., Volonteri M., Natarajan P., Gawiser E. 2011, Nature, 474, 356
- [30] Volonteri M. & Rees M.J. 2005, ApJ, 633, 624
- [31] Volonteri M. & Begelman M.C. 2010, MNRAS, 409, 1022
- [32] Willott C. J. et al., 2010a, AJ, 139, 906
- [33] Xue Y.Q. et al. 2011, ApJ, in press, arXiv:1105:5643